IN VIVO VISUALIZATION OF METASTASIS OF HUMAN BREAST CANCER CELLS LABELED WITH QUANTUM DOTS IN MICE

MASAAKI KAWAI [1)†], HIDEO HIGUCHI [2)], TOMONOBU M. WATANABE [2)], HIROSHI TADA [1)], NORIAKI OHUCHI [1)]

1) Tohoku University Graduate School of Medicine, Division of Surgical Oncology, 1-1, Seiryo-cho, Aoba-ku, Sendai, Miyagi, 980-0801, Japan

2) Biomedical Engineering Research Organization, Tohoku University, Engineering research Lab complex, 6-6-11 Aramaki, Aoba–ku, Sendai, Miyagi, 980–8578, Japan

Semiconductor quantum dots (QDs) are now thought to be as new adjuncts of fluorescence bioprobes for medical applications, especially for cancer imaging. Liver metastasis is reported to be seen in half of the breast cancer patients and is recognized as life-threatening condition. Metastatic processes of the breast cancer cells are recognized as follows; detachment of cancer cells from the primary tumor, intravasation, interactions with endothelial cells and extravasation. Early events in metastasis are thus far not easy to be detected because of the difficulties in identification of single cancer cell or micrometastasis in tissue. To get over these problems, we used human invasive breast cancer cell line, MDA-MB231 which expresses Epidermal Growth Factor Receptor (EGFR) with QDs conjugated with EGFR Antibody for cancer cell imaging. The QDs conjugated with EGFR-Antibody labeled the membrane receptor of MDA-MB231 cells under conjugation, giving ability to image cancer cells *in vivo* under laser scanning confocal microscopy, with evading autofluorescence of the background liver tissue. We made Qdot-EGFR-Antibody labeled tumor cells and inoculated them into the portal veins of BALB/c nu/nu nude mice and observed their livers with intravital imaging system using laser scanning confocal microscopy, initially after injection, the accumulation of the complexes into sinusoids of the liver was observed, suggesting that single cancer cell metastasis in the liver may be visualized on the basis of this experiments.

Keywords: Quantum dot breast cancer, Epidermal growth factor receptor, Intravital tracking, Metastasis, Quantum dots breast cancer.

† Masaaki Kawai has been a Tohoku University 21COE Program Research Assistant from 2004 to 2006.

1. Introduction

Semiconductor quantum dots (QDs) have unique electrical and optical properties such as: high quantum yields, narrow emission bands, high absorbancy, large Stoke's shift, high resistance to photobleaching and can provide excitation of several different emission colors using a single excitation wavelength [1]. Quantum dots exhibit an electronic structure between bands and bonds resulting in a direct correlation between size and emitted wavelength: as the size of the quantum dot decreases, the emitted wavelength. This property enables quantum dots to be designed to emit at a wavelength of interest.

The above properties of quantum dots make them an ideal choice for cellular labeling and in vivo labeling. The narrow emission spectrum without the long tail at red wavelengths characteristic of dyes reduces or eliminates spectral cross talk in detection. The large Stoke's shift enables fluorescent signals from the QDs to easily be separated out from scattered excited light. The fact that nanoparticles are similar in size scale (<5 nm) to common biomolecules makes them ideal for applications such as bioconjugation [2]. A final attractive quality of quantum dots is that they can be synthesized to emit within a spectral region, 600–1300nm, which has been demonstrated as best suited for biological imaging due to high physiological transmissivity [3]. The main benefit of using near IR light is an increased penetration depth due to the low extinction coefficients of hemoglobin, melanin, and water, three prominent skin chromophores, in the near IR region as well as the ability to filter out the signal from excitation light [4].

Despite the many advantages of quantum dots as compared to conventionally used fluorophore dyes, their biological applications have been hampered by their inherently low solubility in water. Recently, new chemical strategies have been established for rendering the quantum dots soluble in various biological solvents enabling their use in biological imaging [5].

Several groups have successfully demonstrated the specific targeting of Qdots in cellular systems as well as the ability to detect the signal from Qdots in cellular labeling, using combination of Qdots linked to a humanized anti-Her2 antibody to label Her2, a breast cancer marker, on the surface of fixed and live cancer cells. The Qdot conjugates were shown to specifically and effectively label the molecular targets [6].

In the last decade, enormous progress has been made to understand the molecular events that accompany carcinogenesis. The identification of unique molecular markers of cancer, such as Epidermal Growth Factor Receptor (EGFR), and the associated processes they modulate allow direct targeting and interrogation of these markers by optical tags [7]. The EGFR is a 170-kDa

transmembrane receptor tyrosine kinase that stimulates the proliferation of a wide variety of animal cell types. EGFR is expressed ubiquitously in cells and is overexpressed in human malignancies including breast cancer. The over-expression of EGFR has been correlated with many processes related to cancer, including uncontrolled cell proliferation, autocrine stimulation of tumor growth by tumors producing their own growth factors and prevention of cellular apoptosis.

Liver metastasis is reported to be seen in half of the breast cancer patients and is recognized as life-threatening condition. Metastatic processes of the breast cancer cells are recognized as follows; detachment of cancer cells from the primary tumor, intravasation, intial arrest, interactions with endothelial cells and extravasation [8]. Early events in metastasis are thus far not easy to be detected because of the difficulties in identification of single cancer cell or micrometastasis in tissue.

In this experiment, we used human invasive breast cancer cell line which expresses Epidermal Growth Factor Receptor (EGFR) with Qdots conjugated with EGFR Antibody for *in vivo* cancer cell imaging as a model of breast cancer liver metastasis. The Qdots conjugated with EGFR-Antibody labeled the membrane receptor of MDA-MB231 cells under conjugation, giving an ability to image cancer cells *in vivo* under laser scanning confocal microscopy, with evading autofluorescence of the background liver tissue.

2. Material and Methods

2.1. *Qdot-Antibody conjugations*

QDs were conjugated to EGFR-Antibody (GeneTex, Inc. TX, USA) with a Qdot 705 Antibody Conjugation Kit (Quantum dot corporation, Hayward, CA) via poly ethylene glycol (Mw. 2000) and SMCC-crosslinkers. The final concentration of Qdot-EGFR-Antibody complexes was determined by measuring the conjugate absorbance at 550 nm and using an extinction coefficient of 1,700,000 $M^{-1}cm^{-1}$ at 550 nm.

2.2. *Cell line and In vitro imaging*

The human breast cancer cell line, MDA-MB231 which expresses EGFR and is sensitive to EGFR-Antibody. MDA-MB231 cells were cultured in Leibovitz's L-15 Medium supplemented with 10% fetal bovine serum. The cells were incubated in the two glass bottom dishes for 24 hours supplemented with 1mL

Leibovitz's L-15 Medium. After incubation, each cells were conjugated to 1nM Qdot-EGFR-Antibody complexes or 1nM Qdots, respectively for 5 minutes, washed in phosphate-buffered saline (PBS) twice and observed.

2.3. *In vivo imaging*

A suspension of MDA-MB231 (1 x 10^6 cells) was conjugated with Qdot-EGFR-Antibody complexes, prepared as mentioned above, at the concentration of 1nM for 10 minutes, centrifuged at 200 x g for 5 min and washed in phosphate-buffered saline (PBS) twice and suspended in a volume of 100 μl Leibovitz's L-15 Medium. Then inoculated to the portal vein of the female BALB/c nu/nu mice at 5-6 weeks of age (Charles River Japan, Yokohama, Japan) in a volume of 100 μl.

The mice were placed under anesthesia by injection of ketamine and xylazine mixture intraperitoneally at a dosage of 95 mg/kg and 5 mg/kg, respectively. After Qdot-EGFR-Antibody-MB231 complex were inoculated into the portal vein with an upper median laparotomy incision, we observed their livers with intravital imaging system using laser scanning confocal microscopy, initially after injection. The temperature of mice was maintained at 37 °C by thermo-plate and objective lens heater. All of the mice were maintained in our pathogen-free institutional facilities. All operations on animals were in according with institutional animal use and care regulations.

The optics system for 3D observation was consisted of an epi-fluorescent microscope (IX71, Olympus) [9, 10], a Nipkow lens type confocal unit (CSU10, Yokokawa), an electron multiplier type CCD camera (iXon 887, Andor) and 690nm long pass filter. The object lens (x60, N.A. 1.45) was moved by a piezo actuator with a feedback loop (Nanocontrol). A computer controlled the piezo actuator in synchronization with the image acquisitions in order that the object lens remained within the exposure time of the CCD camera. An area, ~30×30μm^2, was illuminated by a green laser (532 nm, Crystalaser).

2.4. *Histological imaging*

After imaging, the mice were killed by CO_2 overdose. Liver was removed and divided for histological Qdot-EGFR-Antibody-MB231 complex uptake study, fixed in 10% neutral-buffered formalin overnight and then transferred into ethanol before processing and paraffin embedding and examined with an imaging system.

3. Results

3.1. *In vitro imaging*

With Qdot-EGFR-Antibody complexes, cellular membranous region of the MDA-MB231 was observed fluorescently (Fig. 1), but no signals were observed by Qdot alone (Fig. 2). After 1 hour of conjugation with Qdot, no signals were observed *(data not shown)*.

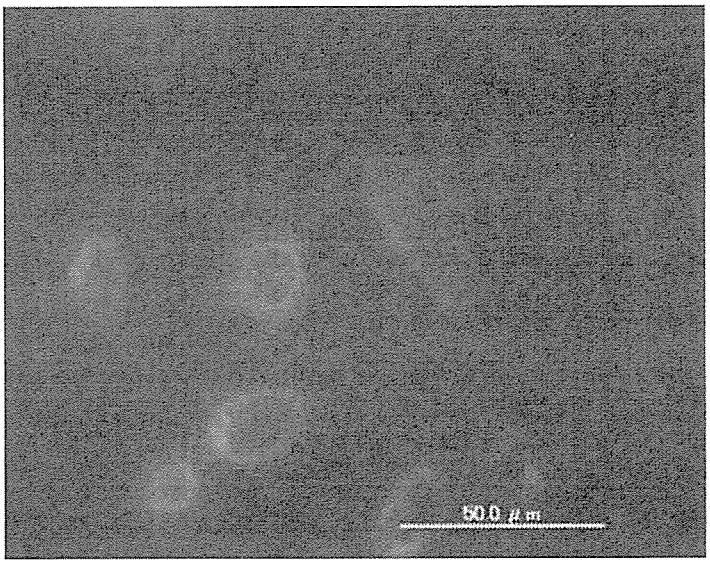

Fig. 1. Fixed breast cancer cell line MDA-MB231 cells were incubated with 1nM Qdot-EGFR-antibody complexes. Cellular membranous region, in which EGFR locates, of the MDA-MB231 cancer cells were observed fluorescently. Scale bar 50μm.

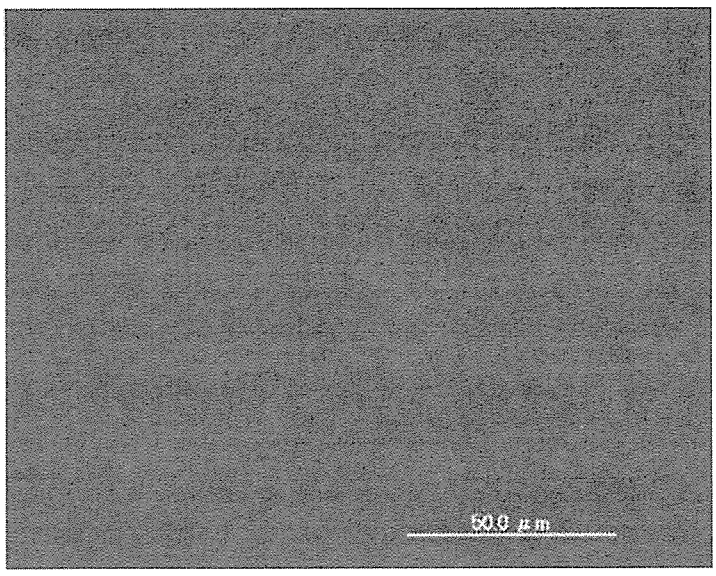

Fig. 2. Fixed breast cancer cell line MDA-MB231 cells were incubated with 1nM Qdot. The cells were not labeled at 1 hour-incubation. Scale bar 50μm.

3.2. *In vivo imaging*

Prior to injection, we observed normal liver of the mouse. Shallow autofluorescence (liver cells, nucleus) was observed, but all of them were very weak compared to the fluorescence of the Qdot (Fig. 3).

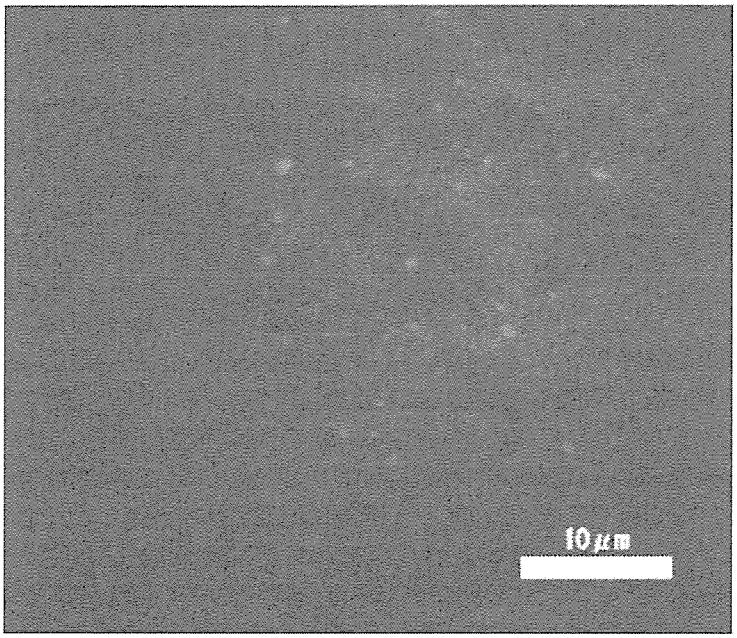

Fig. 3. Intravital imaging of the BALB/c nu/nu normal liver before Qdot-EGFR-antibody-MB231 complexes. Slight autofluorescence of the liver cells and nucleus was observed, but their signal intensity was shallow compared with Qdot fluorescence (*data not shown)*. Scale bar 10μm.

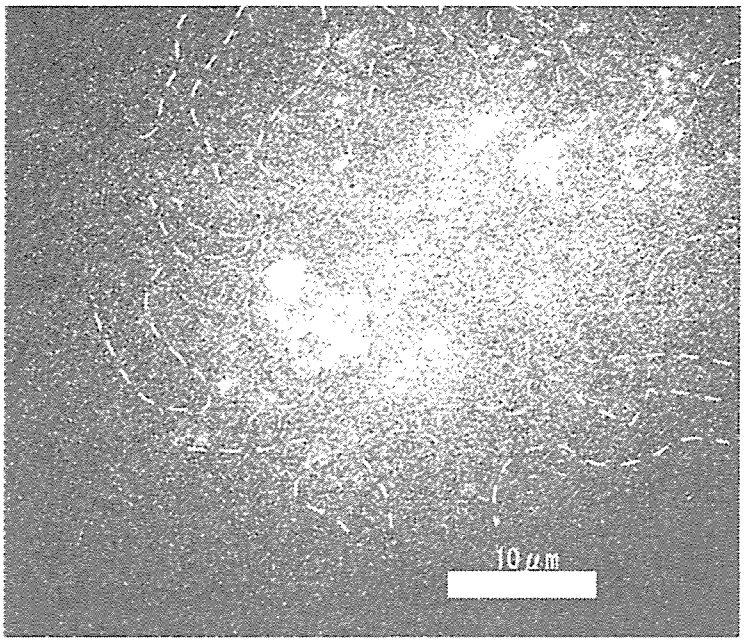

Fig. 4. Intravital imaging of the BALB/c nu/nu liver after Qdot-EGFR-antibody-MB231 complexes injection. A labeled cancer cells was observed (red broken ellipses). White broken line shows outlines of liver cells. Scale bar 10μm.

After Qdot-EGFR-Antibody-MB231 injection, the accumulation of the complexes into sinusoids of the liver was observed. But no cellular movement was observed for 10 minutes observation (Fig. 4).

3.3. *Histological imaging*

After Qdot-EGFR-Antibody-MB231 complexes injection with intravital imaging, the mice were killed by CO_2 overdose. Liver was removed fixed in 10% neutral-buffered formalin overnight and then transferred into ethanol before processing and paraffin embedding and examined with the imaging system. Cancer cells in the sinusoid was observed, but dispersed Qdots are seldom seen (Fig. 5).

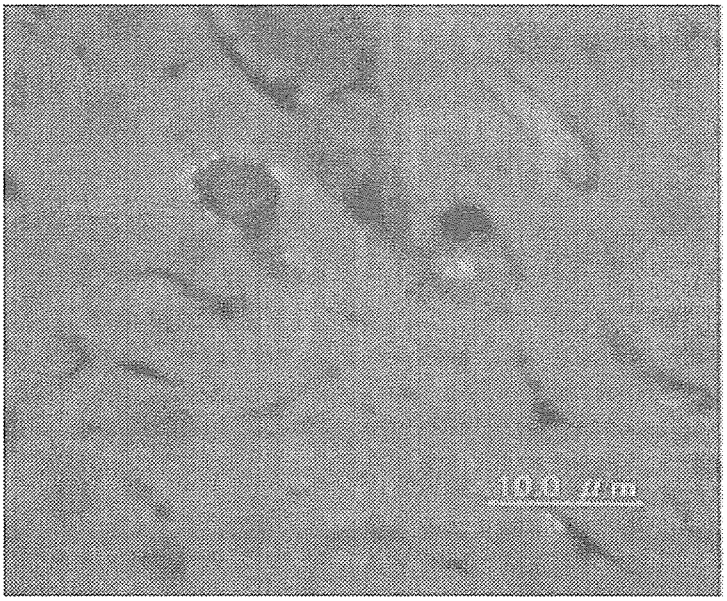

Fig. 5. After Qdot-EGFR-Antibody-MB231 complexes injection, the liver was removed and embedded in paraffin embedding. The imaging system demonstrates cancer cells in the sinusoid (red broken ellipses). Dispersed Qdots were occasionally observed. Scale bar 50μm.

4. Conclusion

In these experiments, we can have MDA-MB231 human cancer cells immunologically stained and the accumulation of the complexes into sinusoids of the liver was observed in intravital imaging system without dissecting the liver tissue *in vivo*, suggesting that these techniques let single cancer cell metastasis in the whole organs be visualized, shedding light on the mechanisms of cancer cell metastasis.

Acknowledgments

We are grateful to the support by Grants-in-aid for Research Project, Promotion of Advanced Medical Technology (H14-Nano-010 and H18-Nano-001), from the Ministry of Health, Labor and Welfare of Japan, and the support by Tohoku University 21st Century Center of Excellence (COE) Program "Future Medical Engineering based on Bio-nanotechnology".

References

[1] Wagnieres G, Star W, and Wilson W. In vivo fluorescence spectroscopy and imaging for oncological applications. *Photochem Photobiol* **68**, 603-632, 1998.

[2] West J, and Halas N. Engineered nanomaterials for biophotonics applications: improving sensing, imaging, and therapeutics. *Annu Rev Biomed Eng* **5**, 285-292, 2003.

[3] Loo C, Lin A, Lee M, Barton J, and Halas N. Nanoshell-enabled photonics-based imaging and therapy of cancer. *Technol Cancer Res Treat* **3**, 33-40, 2004.

[4] Troy T, and Thennadil S. Optical properties of human skin in the near infrared wavelength range of 1000 to 2200 nm. *Gynecol Oncol* **99**, 89-94, 2005.

[5] Chan W, Maxwell D, Gao X, Bailey R, Han M, and Nie S. Luminescent quantum dots for multiplexed biological detection and imaging. *Curr Opin Biotechnol* **13**, 40-46, 2002.

[6] Wu X, Liu H, Liu J, Haley KN, Treadway JA, Larson JP, Ge N, Peale F, and Bruchez1 MP. Immunofluorescent labeling of cancer marker Her2 and other cellular targets with semiconductor quantum dots. *Nat Biotechnol* **21**, 41-46, 2003.

[7] Perez R, Pascual M, Macias A, and Lage A. Epidermal growth factor receptors in human breast cancer. *Breast Cancer Res Treat* **4**, 189-193, 1984.

[8] Ito S, Nakanishi H, Ikehara Y, Kato T, Kasai Y, Ito K, Akiyama S, Nakao A, and Tatematsu M. Real-time observation of micrometastasis formation in the living mouse liver using a green fluorescent protein gene-tagged rat tongue carcinoma cell line. *Int J Cancer* **93**, 212-217, 2001.

[9] Nguyen VT, Kamio Y, and Higuchi H. Single-molecule imaging of cooperative assembly of gamma-hemolysin on erythrocyte membranes. *EMBO J* **22**, 4968-4979, 2003.

[10] Nguyen H, and Higuchi H. Motility of myosin V regulated by the dissociation of single calmodulin. *Nat Struct Mol Biol* **12**, 127-132, 2005.

EFFECTS OF TRASTUZUMAB AND PACLITAXEL IN HER2-OVEREXPRESSING BREAST CANCER

SONGHUA LI [1)†], HIDEO HIGUCHI [2)], NORIAKI OHUCHI [1)]

1) Department of Surgical Oncology, Graduate School of Medicine, Tohoku University, Sendai, Japan

2) Biomedical Engineering Research Organization, Tohoku University, Sendai, Japan

Trastuzumab (anti-HER2 monoclonal antibody) possesses significant clinical activity in breast cancer, and attracts attention as a candidate for molecular target therapy. Furthermore, it was reported that the combination of trastuzumab and paclitaxel improves the anti-tumor effect for metastatic breast cancer. To further understand the molecular basis of trastuzumab and/or paclitaxel in breast cancer therapy, we have visualized these molecules in vivo using quantum dot (Qdot) and GFP. Qdot is relatively new fluorescent dye with longer fluorescent bleaching time and strong fluorescent. We found that trastuzumab blocked HER2 recycling and inhibited the growth of breast cancer cell. Paclitaxel inhibited microtubule depolymerization and mitosis, which induced cell death. Furthermore, the microtubule network which is essential for intracellular transport was fragmented by the combination of trastuzumab and paclitaxel, resulted in the inhibition of intracellular transports. Compared to the individual effect of trastuzumab or paclitaxel, the combination of these two drugs were more effective in inducing cell death in the HER2-overexpressing breast cancer cell.

Keywords: Breast cancer, HER2, Molecular target therapy, Paclitaxel, Quantum dot.

1. Introduction

Overexpression of HER2/neu (c-erbB2), breast cancer growth factor, is reported in 20-30% of patients with breast cancer [1]. Overexpression of HER2 is known for bladder cancer, ovarian cancer, gastric cancer besides breast cancer. It has been reported that when HER2 is overexpressed, chance of metastasis and recurrences increase, and HER2/neu oncoprotein is a prognostic indicator in human breast cancer [2,3].

Trastuzumab is a humanized monoclonal antibody directed against the HER2 protein, which is clinically active treatment in HER2-overexpressing

† Songhua Li has been a Tohoku University 21COE Research Assistant from 2003 to 2006.

metastasis breast cancer [4-7]. The taxanes, paclitaxel and docetaxel, represent two of the most active chemotherapeutic agents for the treatment of patients with breast cancer. Paclitaxel was the first diterpene agent to be developed for clinical use and has demonstrated activity in the treatment of a number of different human cancers. Diterpene chemotherapeutic agents act by inhibiting microtubule disassembly [8]. Paclitaxel is active mainly in the treatment of metastasis breast cancer [9,10]. The combination of trastuzumab and paclitaxel resulted in the highest tumor growth inhibition and had a significantly superior complete tumor regression rate [11-14]. However, a process of trastuzumab and/or paclitaxel response and a structural change of the cancer cell by the combination was not clear in HER2-overexpressing breast cancer cells. Therefore, we have performed this study to visualize alteration of intracellular configuration by combination of trastuzumab and paclitaxel. Our study will be helpful in development of new anticancer drug in the future.

2. Materials and Methods

Cell line: KPL-4 breast cancer cell which overexpressed HER2 protein. KPL-4 cell was cultured in Dulbecco's Modified Eagle Medium (DMEM) supplemented with 5% Fetal Bovine Serum (FBS) at 37℃ in a 5% carbon dioxide atmosphere.

Quantam Dot (Qdot):Trastuzumab was labeled with Qdot705 using Qdot antibody conjugation kit (SC BioSciences Corporation), KPL-4cell was incubated in DMEM supplemented with 5% FBS containing 10nM Qdot-Trastuzumab (QT) , and cultured for 1 hour at 37℃ in a 5% carbon dioxide atmosphere. We changed culture media 1hour later. Cells were observed under confocal microscope equipped with 532nm laser and images were saved in PC for analysis.

Green fluorescent protein (GFP): It is known that paclitaxel inhibits microtubule depolymerization.KPL-4 was lipofected with GFP-tubulin vectoer so that depolymerization of microtubule and trastuzumab transport on microtubule can be visualized. Stably transfected cell was cloned by G418 (400ug/ml) selection.GFP-Tubulin-KPL-4 cell was cultured as KPL-4 cell. 20nM paclitaxel or combination of 100nM transtuzumab and 5nM paclitaxel was added to culture media, and incubated for 48 hours. These cells and control cells were observed under confocal microscope equipped with 488nm laser and images were saved in PC for analysis.

3. Results

1. When 10nM Qdot-Trastuzumab (QT) was added to culture media with KPL-4 cells, QT did localized at cell membrane (yellow line, Fig. 1A). This result showed the binding of QT and membrane transfix protein HER2 in KPL-4 breast cancer cell. Twenty-four hours later, QT was completely transported intracellularly and localized at perinucleus region (Fig. 1B). This showed that QT was transported intracellularly by motor protein.

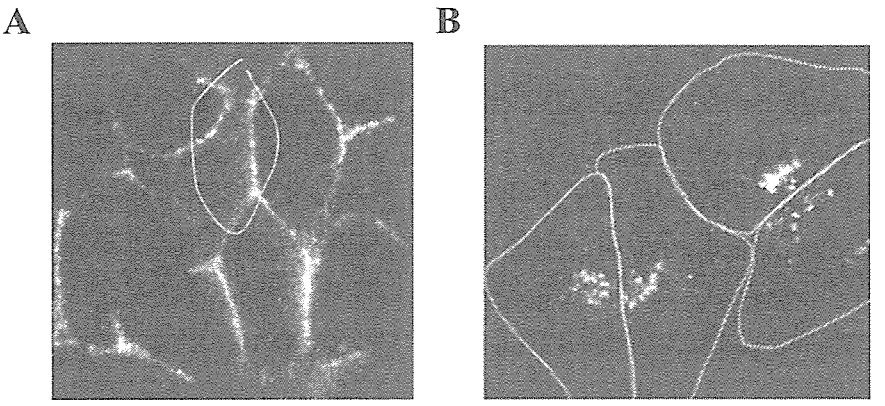

Fig. 1. Localization of 10 nM QT in a KPL-4 cell by a confocal laser scanning microscope (yellow line show a position of cell membrane). (A) One hour after adding QT. (B) After 24 hours.

2. When KPL-4 cell was treated with paclitaxel and incubated with QT for 1 hour, QT localized to cell membrane as same as Fig. 1A. However, 24 hours later, QT scattered in cytoplasm. This suggests there was inhibition of intracellular transport pathway by paclitaxel.

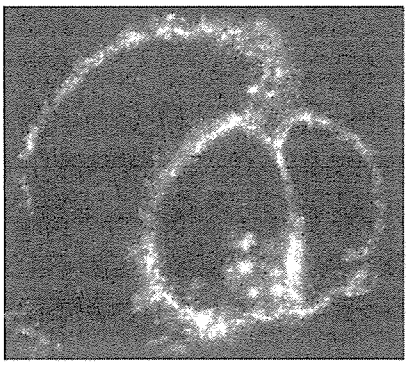

Fig. 2. KPL-4 cells treated in 20nM paclitaxel for 24 hours, showing localization of 10nM QT in a cell detected by the confocal laser scanning microscope.

3. A characteristic microtubule form was observed distinctly in the KPL-4 cell expressing GFP-Tubulin. On the other hand, cells incubated in 20nM paclitaxel for 48 hours showed multinuclei, and consistency of microtubule at cell

membrane periphery became high. However, form of microtubule did not have a change. In comparison with control, there were many dead cells. It is resulted by inhibition of mitosis of paclitaxel that became multinuclear, and it seems that the reason why microtubule consistency around cell membrane became high is that microtubule was pushed aside by the polynuclear that gathered in the middle of cell. Compared with control or 20nM Paclitaxel treated cells, short microtubule was observed in cells treated with 60nM trastuzumab and 5nM Paclitaxel.

4. Discussion

When cells were treated by Trastuzumab alone, QT (Qdot-Trastuzumab) bind to membrane transfix protein HER2, and it was transported intracellularly by motor protein (myosin, dynein) and localized at the perinucleus region (Fig. 1B). This result indicates that trastuzumab inhibits recycling of HER2, and inhibited the returning of HER2 to cell membrane.

QT scattered in cytoplasm, in combination trastuzumab and paclitaxel.This suggests that there was inhibition of intracellular transport pathway. Paclitaxel is reported to inhibit depolymerization of microtubule and inhibit mitosis thus result in anticancer activity [9,10]. However, form of microtubule was not a change when treated 20nM Paclitaxel alone. Compared with control, short microtubule was observed in cells treated with 60nM trastuzumab and 5nM paclitaxel. The microtubule was fragmented in combination trastuzumab and paclitaxel, which did not happen in paclitaxel alone. It is thought that QT is transported intracellularly by motor protein (Fig. 1B). It appears that the higher consistency of microtubule at cell membrane periphery inhibited motor protein. Motor protein draws out microtubule in the microtubule transportation network that became overcrowded and causes non-coordinate action, so the result is thought there is a possibility that microtubule was fragmented.

It was found that trastuzumab blocked HER2 recycling and inhibited the growth of breast cancer cell. Paclitaxel inhibited microtubule depolymerization and mitosis, and was able to ascertain that a cell dies. Furthermore, the microtubule network for intracellular transport was fragmented by the combination of transtuzumab and paclitaxel, resulting in the inhibition of intracellular transports. Compared to the individual effect of trastuzumab or paclitaxel, the combination of these two drugs were more effective in the HER2-overexpressing breast cancer cell.

Because we were able to visualize an intracellular change by combination of trastuzumab and paclitaxel, we would like to quantify Qdot in breast cancer cell in future to study if the effect of these two drugs is additive or synergistic.

We will develop new immunostaining method of cell and tissue using Qdot in the future and want to aim at application to quantitative carcinomatous pathological diagnosis and cancer therapy for high sensitivity.

Acknowledgments

KPL-4 breast cancer cell was a kind gift from Mr. J Kurebayashi (Kawasaki Medical School, Kurashiki, Japan). We would like to thank Drs. Tomonobu Watanabe and Motoshi Kaya at Biomedical Engineering Research Organization, Tohoku University for help with microscopy, imaging, and discussion. Songhua Li acknowledges the support of Tohoku University 21 COE Program "Future medical engineering based on bio-nanotechnology". We are grateful to the support by Grants-in-aid for Research Project, Promotion of Advanced Medical Technology (H14-Nano-010 and H18-Nano-001), from the Ministry of Health, Labor and Welfare of Japan, and the support by Tohoku University 21st Century Center of Excellence (COE) Program "Future Medical Engineering based on Bio-nanotechnology".

References

[1] Slamon DJ, Clark GM, Wong SG, Levin WJ, Ullrich, and McGuire WL. Human breast cancer: Correlation of relapse and survival with amplification of the HER2/neu oncogene. *Science* **235**, 177-182, 1987.

[2] Wright C, Angus B, Nicholson S, Sainsbury JRC, Cairns J, Gullick WJ, Kelly P, Harris AL, and Wilson Horne CH. Expression of c-erbB-2 oncoprotein: A prognostic indicator in human breast cancer. *Cancer Res* **49**, 2087-2090, 1989.

[3] McCann AH, Dervan PA, O'Regan M, Codd MB, Gullick WJ, Tobin BM, and Carney DN. Prognostic significance of c-erbB2 and estrogen receptor status in human breast cancer. *Cancer Res* **51**, 3296-3303, 1991.

[4] Baselga J, Tripathy D, Mendelsohn J, Baughman S, Benz CC, Dantis L, Sklarin NT, Seidman AD, Hudis CA, Moore J, Rosen PP, Twaddell T, Henderson IC, and Norton L. Phase II study of weekly intravenous recombinant humanized anti-p185HER2 monoclonal antibody in patients with HER2/neu-overexpressing metastatic breast cancer. *J Clin Oncol* **14**, 737-744, 1996.

[5] Pegram MD, Lipton A, Hayes DF, Weber BL, Baselga JM, Tripathy D, Baly D, Baughman SA, Twaddell T, Glaspy JA, and Slamon DJ. Phase II study of receptor-enhanced chemosensitivity using recombinant humanized anti-p185HER2/neu monoclonal antibody plus cisplatin in patients with HER2/neu-overexpressing metastatic breast cancer refractory to chemotherapy treatment. *J Clin Oncol* **16**, 2659-2671, 1998.

[6] Cobleigh MA, Vogel CL, Tripathy D, Robert NJ, Scholl S, Fehrenbacher L, Wolter JM, Paton V, Shak S, Lieberman G, and Slamon DJ. Multinational study of the efficacy and safety of humanized anti-HER2 monoclonal antibody in women who have HER2-overexpressing metastatic breast cancer that has progressed after chemotherapy for metastatic disease. *J Clin Oncol* **17**, 2639-2648, 1999.
[7] Brenner TL and Adams VR. First MAb approved for treatment of metastatic breast cancer. *J Am Pharm Assoc* **39**, 236-238, 1999.
[8] Rowinsky EK. Paclitaxel pharmacology and other tumor types. *Semin Oncol* **24** (Suppl 19), 1-12, 1997.
[9] Seidman AD, Tiersten A, Hudis C, Gollub M, Barrett S, Yao TJ, Lepore J, Gilewski T, Currie V, Crown J, *et al.* Phase II trial of paclitaxel by 3-hour infusion as initial and salvage chemotherapy for metastatic breast cancer. *J Clin Oncol* **13**, 2575-2581, 1995.
[10] Davidson NG. Single-agent paclitaxel as first-line treatment of metastatic breast cancer: the British experience. *Semin Oncol* **23** (Suppl 11), 6-10, 1996.
[11] Baselga J, Norton L, Albanell J, Kim YM, and Mendelsohn J. Recombinant humanized anti-HER2 antibody (Herceptin) enhances the antitumor activity of paclitaxel and doxorubicin against HER2/neu overexpressing human breast cancer xenografts. *Cancer Res* **58**, 2825-283, 1998.
[12] Pegram M, Hsu S, Lewis G, Pietras R, Beryt M, Sliwkowski M, Coombs D, Baly D, Kabbinavar F, and Slamon D. Inhibitory effects of combinations of HER-2/neu antibody and chemotherapeutic agents used for treatment of human breast cancers. *Oncogene* **18**, 2241-2251, 1999.
[13] Dieras V, Beuzeboc P, Laurence V, Pierga JY, and Pouillart P. Interaction between Herceptin and Taxanes. *Oncology* **61**, 43-49, 2001.
[14] Merlin JL, Barberi-Heyob M, and Bachmann N. In vitro comparative evaluation of trastuzumab (Herceptin) combined with paclitaxel (Taxol) or docetaxel (Taxotere) in HER2-expressing human breast cancer cell lines. *Ann Oncol* **13**, 1743-1748, 2002.

NANO-SIZED FLUORESCENT PARTICLES AS NEW TRACERS FOR SENTINEL NODE DETECTION: AN EXPERIMENTAL MODEL FOR DECISION OF APPROPRIATE SIZE AND WAVELENGTH

MORIO NAKAJIMA [1)†], MOTOHIRO TAKEDA [1)], MASAKI KOBAYASHI [2)], NORIAKI OHUCHI [1)]

1) Department of Surgical Oncology, Graduate School of Medicine, Tohoku University, 1-1 Seiryo-machi, Aoba-ku, Sendai 980-8574, Japan

2) Department of Electronics, Tohoku Institute of Technology, 35-1 Kasumi-cho, Yagiyama, Taihaku-ku, Sendai 982-8577, Japan

The concepts of made-to-order and low-invasiveness medicine are becoming widely accepted. A treatment for cancer, with minimum invasive surgery without lymph nodes dissection based on sentinel lymph node (SN) navigation surgery would adhere to these concepts. Dyes and /or radioisotopes are employed for SN detection in standard methods, however, each detection method has advantages and disadvantages. To make up for the disadvantages, we aimed at developing a new non-invasive method using fluorescent beads of uniform nano-size that could efficiently visualize SN from outside the body and conducted experiments to determine the appropriate size and fluorescent wavelength. We examined various bead sizes and fluorescent wavelengths. The sizes were 20, 40, 100 and 200nm. The fluorescent peak wavelengths of the beads were Yellow-green (515 nm), Dark red (680 nm), Far red (720 nm) and Infrared (755 nm). The beads were subcutaneously injected into the foot pad of the hind leg of a rat, and followed by laser scanning of the inguinal area for fluorescence observation. The beads exhibited different times for the fluorescence detection according to their sizes and wavelength. The 40 nm beads were considered to be the most appropriate size for SN detection in rats. The wavelength of near infrared was effective of avoiding attenuation by the tissue. In conclusion, we confirmed that uniformly nano-sized fluorescent beads have the potential to be an alternative to existing tracers in the detection of the SN in animal experiments if we select the appropriate particle size and wavelength.

Keywords: Cancer metastasis, Fluorescent beads, Nanotechnology, Sentinel node biopsy.

1. Introduction

The sentinel node (SN) is the first lymph node on the lymphatic drainage pathway from the cancerous tumor. In cases where the SN has a metastasis,

† Morio Nakajima was a Tohoku University 21COE Research Assistant from 2002 to 2004.

there is the possibility of another positive node. When the SN is negative for metastasis, we can consider that there will be no other positive node and lymph nodes dissection (LND) is not necessary except for the SN. It leads to the avoidance of the functional or organic complication after LND. Preventive and systematic LND in cancer surgery has been accepted as a standard technique for over one hundred years, however, the modern concept of minimizing the invasiveness of medical treatment is changing surgical procedures. This SN navigation surgery presents a new choice to patients as a made-to-order medical treatment. There are two major methods for detection of SN using tracer molecules: one is a dye method in which iso-sulfan blue: the other is a radio isotope (RI) method in which ^{99m}Tc with phytic acid is used severally for example. They are subcutaneously injected at the periphery of the tumor, and then the SN can be identified through the tracer accumulation [1-4]. High sensitivity in the detection of a SN can be achieved using these two methods together. However, there are disadvantages for each method. The dye method requires some great skill, and cannot be detected without a skin incision. The RI method requires radioactive agents; therefore it can only be performed at certain hospitals because of the regulations for handling them.

To make up for the disadvantages, we designed fluorescent nano-sized beads as a new alternative tracer. There are many factors that might influence their movement in the lymphatic system when particles are subcutaneously administered *in vivo*. We noted the particle size as the most important factor. Small sized particles immediately move into lymphatic capillaries and pass through the interstices of the endothelial cells from the interstitial tissue. Large sized particles are carried by macrophages after phagocytosis [5]. It is necessary to determine the appropriate size for SN accumulation by passive lymphatic movement.

We used nanosized fluorescent beads of extremely narrow diameter distribution. Autofluorescence, optical absorption and scattering in living tissue are the factors that prevent us from optical measurement deep in a living body. Therefore we need to use a light source with an appropriate wavelength for effective excitation. In this study, we examined the detection of SNs from outside the body using various particle sizes and wavelengths to determine the optimum size and wavelength. These data should aid the adoption of a fluorescence measurement method in the future.

2. Materials and Methods

2.1. *Fluorescent beads*

We used "FluoSpheres®" manufactured from high –quality, ultraclean polystyrene microspheres by Molecular Probe Inc. (OR, USA). There are various bead sizes and fluorescent colors. We selected beads of sizes 20, 40, 100, and 200 nm and fluorescent colors of Yellow-green (YG) (excitation/emission maxima at 505/515 nm), Dark red (DR) (660/680 nm), Far red (FR) (690/720 nm) and Infrared (IR) (715/755 nm). The beads diameter distribution is very small, that is, 0.02 ± 0.004μm in 20nm size (*i.e.* within 20% error) and 0.1 ± 0.005μm in 100nm (*i.e.* within 5% error).

2.2. *Animals*

We used male, 6-9 weeks old, Donryu rats (180～250 g) in the experiment.

2.3. *Instrumentation*

We designed a laser scanning fluorescence detection system, which consists of three lasers, a resonant scanner (resonant frequency/200 Hz), a rotational pulse-stage and a CCD camera. We used a diode pumped solid-state blue laser (wavelength 473nm, output power 7mW) as the excitation source of YG fluorescent beads. For excitation of DR, FR, and IR fluorescent beads, we used a He-Ne laser (632.8 nm, 14.6 mW) or a laser diode (657 nm, 3.56 mW). The inguinal and femoral areas were continuously irradiated and scanned over an area of 30 × 50 mm. The fluorescence image was observed using a CCD camera (XC-EI50, Sony) with an optimum band-pass filter for each fluorescent bead. In addition the spectrum of scanned area was analyzed with spectro-meter.

2.4. *Procedure*

Under ether anesthesia, the hair of rats' lower body was removed to avoid autofluorescence of it. Then 50μl of FluoSpheres® 2% w/vol suspension was subcutaneously injected at the foot pad of the hind leg.

Spectral analysis of fluorescence from rats injected with beads was performed to clarify the signal to noise ratio of fluorescence from beads and autofluorescence. After observation from outside the body (through the skin) for 30-180 minutes, we peeled back the skin at the subcutaneous layer and ascertained the area of lymph nodes with navigation of their specific fluorescence. Then, the lymph nodes were removed, fixed with formalin and

embedded in paraffin. Afterwards histological observation was performed with HE stain to confirm that the tissue was a lymph node.

This experiment was carried out based on the guidelines about animal experiments at Tohoku University, after acknowledgement by the committee on animal experiments. We used the z approximation about two proportions of two independent groups and student's t-test about the mean as statistical analysis methods.

3. Results

3.1. *Particle sizes*

About particle sizes, we conducted the experiment on four types of beads with diameters of 20, 40, 100 and 200 nm. (Table 1-a) In the experiment using 20 nm beads, 22 feet from 13 rats were tested. SNs were detected in 10 feet of 22 (45%) by fluorescence contrast. The time of detection from injection was 0 to 6 minutes. The average time for detection was 2.5 minutes and the median time was 2 minutes. With 40 nm beads, SNs were detected in 50 of 72 feet (69%). The time of detection from injection was 0 to 28 minutes. SNs in 42 feet were detected within 5 minutes. It was the most representative case (84%). The average time was 4.6 minutes and the median time was 3 minutes.

With 100 nm beads, SNs were detected in 2 of 10 feet (20%). The average and median times were both 56 minutes. With 200 nm beads, SNs were detected in 7 of 18 feet (39%). The average time was 127 minutes. The median time was 135 minutes. In the 40 and 20 nm experiments, there was a significant difference in both the "positive rate" and "average time". In the same way, we compared 40 with 100 or 200 nm beads severally (Table 1-a).

3.2. *Fluorescent wavelengths*

About wavelengths, we investigated three excitation and emission wavelengths with the 40 nm beads, Yellow-green (YG), Dark red (DR) and Infrared (IR). Beads of 40 nm in diameter were found to be the most suitable size in the previous experiment.

In the experiment using YG, 10 feet from 5 rats were tested. SNs in 3 of 10 feet (30%) were observed by fluorescence measurement. With DR, SNs in 24 of 31 feet (77%) were observed and with IR, SNs in 23 feet of 31 feet (74%) were observed. DR and IR have advantage of "positive rate of fluorescence detection" as compared with YG (Table 1-b).

4. Discussion

The time of detection from tracer injection and the duration of marking are important for the detection of SNs in practical surgery. It is ideal that the tracer reaches SNs soon after injection and is trapped for a long time without moving to another lymph node. In this experiment, 100 and 200 nm sized beads took too long a time to reach SNs, and the detection time was not reproducible. In contrast, in the case of 20 nm beads we could observe the fluorescence right after injection but they disappeared immediately without staying. Therefore the size of 20 nm was too small for trapping in the SNs. Based on this and the statistical analysis of this experiment (Table 1-a), it was considered that 40 nm sized beads were the most suitable size for detection time and reproducibility. We could confirm that the particle size is important as a physical factor.

Table 1. Results of particle sizes and wavelengths.

a.

diameter	total number of rats (total number of legs)	number of fluorescent legs	positive rate of fluorescence detection	average time to fluorescence detection (minutes)	SE	SD	Mdn
20nm	13 (22)	10	45% *1	2.5 *2	0.6	1.8	2
40nm	40 (72)	50	69% *3 *5	4.6 *4 *6	0.9	7.0	3
100nm	5 (10)	2	20%	56	54	76	56
200nm	10 (18)	7	39%	127	20	53	135

b.

fluorescent wavelength excitation/emission	total of rats (total of legs)	number of fluorescent legs	positive rate of fluorescence detection	average time to fluorescence detection (minutes)	SE	SD	Mdn
Yellow-green 505/515	5(10)	3	30% *7 *8	13	5.4	9.3	10
Dark red 660/680	19(31)	24	77% *9	6.0 *10	1.8	8.8	2.5
Infrared 715/755	16(31)	23	74%	2.1	0.3	1.4	2

(a) Particle size of fluorescent beads. The total number of rats employed in the experiment was 68 (122 legs). *1: p=0.040 (Z=2.05). *2: p=0.032 (t-test). *3: p=0.002 (Z=3.04). *4: sample is too small to analysis. *5: p=0.016 (Z=2.41). *6: p=0.0005 (t-test). (b) Wavelength of fluorescent beads at 40nm. *7: p=0.005 (Z=2.75). *8: p=0.011 (Z=2.52). *9: p=0.766 (Z=0.29). *10: p=0.020 (t-test) (SE: standard error, SD: standard deviation, Mdn: median).

Homogeneous nano-sized beads have an advantage for efficient SN detection compared to existing colloids agents of heterogeneous size. Although the appropriate size for SN detection for human beings is predicted to be 500 nm and the optimum size may be different between animal species, the appropriate size should be determined for humans with very accurately measured nano-sized beads of strictly same dimensions. We can select the size to match the purpose for detection time or trapping duration if we can determine the relationship between particle size and detection time or trapping duration.

Hemoglobin in blood and water is known to be a strongly absorptive substance in living tissue. Hemoglobin absorbs light in the range of visible light below 650 nm, and water absorbs light above 1100 nm. But in the near infrared range between 650 and 1100 nm, the absorption of light in living tissue is minimum. This range is called the 'optical window'. Besides collagen, NADH and FAD are substances that *in vivo* have the fluorescent wavelengths in the range of 400 to 500 nm. So, from this point of view, NIR range has the advantage for the fluorescence measurement. In these experiments four different fluorescent wavelengths 515, 680, 720 and 755 nm were studied. DR and IR were more sensitive than YG in the detection rate experiments with 40 nm beads (Table 1-b *7, 8). Additionally, autofluorescence of the skin was strong and prevented measurement at the wavelength of YG.

There was no significant difference in "positive rate", but in "average time" between DR and IR (Table 1-b). However, spectral analysis of DR and IR showed that IR has a higher signal-to-noise ratio compared than DR.

There are two forms of transportation mechanism regarding a particle material to lymphatic system that is injected into tissue space. One is physical and active extracellular transportation; a particle passes through lymph capillaries. The other one is intracellular transportation of a particle. Foreign materials shift to the lymph capillaries after phagocytosis of particle. It is experimentally reported that extracellular transportation was overwhelmingly dominant within 24 hours after colloids injection to subcutis, whereas intracellular transportation was observed after one week [6].

An investigation of *in vivo* dynamics of tracers is important in SN biopsy. It is reported that lymph node was detected by protected graft copolymer (PGC) combined with Cy5.5, or methoxypolyethyleneglycol (MPEG)-poly-L-lysine combined with Cy5.5 as a tracer [7-9]. The report shows that most of the subcutaneously injected tracer remained at an injected site without transportation, and some of them transferred to lymph nodes and remained. After intravenously injected, the tracer distributed in reticuloendothelial system including liver or spleen other than lymph node.